Journal of Applied Polymer Science

Comparison of Direct Solvents for Regenerated Cellulosic Fibers via the Lyocell Process and by Means of Ionic Liquids

D. Ingildeev,[1] F. Effenberger,[2] K. Bredereck,[2] F. Hermanutz[1]
[1]ITCF Denkendorf, Körschtalstraße 26, Denkendorf D-73770, Germany
[2]Stuttgart University, Pfaffenwaldring 55, D-70569 Stuttgart, Germany
Correspondence to: F. Effenberger (E-mail: franz.effenberger@oc.uni-stuttgart.de)

ABSTRACT: Because new technology using ionic liquids (ILs) for cellulose processing enables the spinning of cellulose with various techniques, the resulting fiber property profiles differ significantly, depending on the process parameters. ILs are thermally stable, nontoxic, environmentally friendly solvents and dissolve cellulose directly; this leads to a high flexibility in the complete process chain for man-made cellulosics. A comparison of the manufacture of cellulosic fibers according to the Lyocell process and by means of ILs is presented. The rheological behavior of the spinning dopes, the structures, and the physical textile properties of the prepared fibers were determined. The fibers spun from solutions of cellulose in *N*-methyl morpholin-*N*-oxide monohydrate, 1-ethyl-3-methyl imidazolium acetate, and 1-ethyl-3-methyl imidazolium diethyl phosphate were compared. © 2012 Wiley Periodicals, Inc. J. Appl. Polym. Sci. 000: 000–000, 2012

KEYWORDS: fibers; morphology; properties and characterization; structure; WAXS

Received 7 November 2011; accepted 8 August 2012; published online
DOI: 10.1002/app.38470

INTRODUCTION

Cellulose decomposes below its melting point and, therefore, cannot be processed in the melt. Furthermore, cellulose is not soluble in conventional solvents because of its complex supramolecular structure, which is formed of intermolecular and intramolecular hydrogen bonds.[1–5] Moreover, there is strong evidence for cellulose being significantly amphiphilic, with hydrophobic interactions between anhydroglucose units.[6–8] Therefore, the production of man-made cellulosic fibers requires either chemical derivatization of the cellulose or dissolution in a suitable solvent. Approximately 95% of the production volume of man-made cellulosic fibers is produced by the viscose process, which involves the derivatization of alkali cellulose with carbon disulfide to give cellulose xanthate.[5,9–12] The cellulose xanthate is dissolved in sodium hydroxide to form a viscous dope (ca. 8 wt %), which is subsequently spun into a spin bath containing sulfuric acid, sodium sulfate, and zinc salts to give regenerated cellulosic fibers. The viscose process is characterized by a high tunability, which results in a large and a variable range of targeted fiber properties. Despite continuous improvements in the last decades, the viscose process still has severe disadvantages, such as high water consumption, contamination of the atmosphere, and process water with toxic and unpleasant sulfur compounds. Because of the increasing investment in environmental protection, the application of carbon disulfide free, direct-solution systems for cellulose has been investigated extensively, but only the Lyocell process has become an important commercial alternative.[13] The Lyocell process is characterized by direct dissolution of wood pulp in *N*-methyl morpholin-*N*-oxide monohydrate (NMMO·H_2O) at concentrations of 10–16 wt % and is used to produce high-strength fibers with excellent tenacity in the wet state.[5,14–20] Despite many advantages, including a unique property profile and an environmentally friendly process, Lyocell fibers are not a full substitute for viscose fibers at this point. The main reason for this is the strong tendency of the fibers to undergo wet fibrillation, which can lead to undesired rope-marking effects and partial damage during rope finishing/dyeing or in garment washing.[5,21–23] Moreover, the solvent *N*-methyl morpholin-*N*-oxide (NMMO) is thermally unstable at process temperatures above 100°C, especially in the presence of heavy metals. Radical decomposition/degradation, deoxygenation, and the Polonovski reaction are the main side reactions.[24] The dissolution process of cellulose in NMMO also has some disadvantages with regard to chemical alterations involving decomposition/degradation reactions of NMMO and cellulose, and this requires a major investment in safety technology.[25–28]

Significant efforts have been made to find new processes to produce man-made cellulosic fibers with a performance profile compared to viscose rayon but in an environmentally friendly and efficient manner.[29–33] This can be done with ionic liquids

© 2012 Wiley Periodicals, Inc.

(ILs) for the dissolution of cellulose, which enables fiber fabrication in a manner very similar to both the viscose and NMMO processes. ILs are salts with melting points below 100°C.[29–36] A great number of possible cation and anion combinations has led to the proposal of numerous applications, including catalysis, extraction, organic synthesis, and metal and polymer processing.[32,34] The possible selection of cations and anions has a strong impact on the physical properties of ILs and often defines their stability. The dissolution process of cellulose in ILs is, in general, controlled by the selection of the anion. Anions such as halides, carboxylates, or phosphates prevent the formation of intramolecular and intermolecular hydrogen bonds between the polymer chains and sheets.[37–40] 1-Ethyl-3-methyl imidazolium acetate ([EMIM][OAc]) is the most preferred IL for cellulose processing.[30,31] In addition, after detailed screening with different ILs at ITCF, 1-ethyl-3-methyl imidazolium diethyl phosphate ([EMIM][DEP]) was found to be of practical importance with regard to the spinning of highly viscous cellulosic solutions with an air gap.[41,42] The ionic liquids with melting points below room temperature (RTILs) used in this study had many significant advantages for processing cellulose into fibers. [EMIM][OAc] and [EMIM][DEP] are thermally stable, nontoxic solvents (no significant acute toxical data were identified in literature) and have a very high dissolution ability for cellulose; they provide a high flexibility for the complete process chain for man-made cellulosics. Moreover, laboratory-scale investigations have shown that ILs used in cellulose processing can be recovered almost entirely (>99.5%) after use in the process, and this has indicated their high durability.[34,43,44]

Because IL technology enables the processing of cellulose with different spinning techniques, the resulting fiber property profiles differ significantly depending on the process chosen. Although the conventional wet-spinning process produces fibers with properties close to those of standard viscose fibers, processing in a dry–wet-spinning process (with an air gap) gives fibers with property profiles comparable to those given by the Lyocell process.[30,45,46]

In this article, we discuss the influence of direct solvent systems, including NMMO·H_2O, [EMIM][OAc], and [EMIM][DEP], on the complete processing chain of man-made cellulosic fibers.

To assess the value of the novel technology using ILs, the preparation of spinning dopes, dissolution behavior, spinning process, fiber structure, and physical textile properties of the manufactured fibers were evaluated and compared to those from the NMMO process with analogous spinning conditions.

EXPERIMENTAL

Materials

Two cellulose samples were used in this study. Cotton linters (DP 759 with an α-cellulose content of 97.0%) and eucalyptus sulfite pulp (DP 592 with an α-cellulose content of 94.1%). The investigations of the dissolution behavior in the kneader under air and N_2, respectively, were performed with cotton linters. The comparison of the rheological properties of cellulose solutions in NMMO and ILs and the evaluation of cellulose processing into fibers were accomplished with eucalyptus sulfite pulp.

The ILs were supplied by BASF. An approximately 50 wt % aqueous NMMO solution was purchased from Merck.

Dissolution Processes of Cellulose in ILs and NMMO·H_2O

The milled pulp was dried at 105°C, added to a preheated IL, and mixed in a kneader at 85°C for 2 h. After complete dissolution of the cellulose, the spinning dope was filtered, degassed *in vacuo* at 85°C, and then supplied to the spinning device.

To obtain a cellulose spinning dope in NMMO·H_2O, the milled pulp was dried at 105°C and subsequently suspended in an aqueous NMMO solution with 40 wt % water in a reactor equipped with a wing stirrer. The water content was determined by Karl Fischer titration with a Mitsubishi CA-02 moisture meter. The suspension was stabilized by 0.06 wt % isopropyl gallate (propyl-3,4,5-trihydroxybenzoate) and 0.04 wt % NaOH. Thereafter, the excess water was distilled off at elevated temperatures until the desired composition of cellulose/NMMO·H_2O was obtained. After the complete dissolution of cellulose and after the NMMO·H_2O, the spinning dope was filtered and then supplied to the spinning device.

Rheology of the Spinning Dopes

The rheological measurements were accomplished with a Rheometrics (SR 500) rheometer equipped with parallel-plate geometry and a Peltier temperature-control system. The shear rates varied between 0.1 and 100 s^{-1}. The diameters of the plates were 25 mm, and the gap between them was 1 mm. The viscoelastic properties of the spinning dopes were studied by dynamic oscillatory experiments at temperatures between 30 and 100°C; this provided the determination of the storage modulus (G'), the loss modulus (G''), and the complex viscosity (η^*). With the principle of frequency–temperature superposition, master curves were obtained. The zero-shear viscosity (η_0) was calculated by the Carreau model.

Filtration

The filtration of the low-viscous spinning dopes was accomplished with a laboratory-scale filtration vessel (2 L) purchased from Karl Kurt Juchheim Laborgeräte GmbH with a polyester nonwoven fabric with a mesh size of 5 μm at 90°C and 2 bar.

The filtration of the high-viscous spinning dopes was accomplished with a metallic tissue with a mesh size of 42 μm.

Spinning Trials

A 6 wt % cellulose solution in [EMIM][OAc] was spun by means of a Fourné laboratory-scale wet spinning device at 90°C. The fibers were extruded with a spinneret with a hole diameter of 0.04 mm containing 1000 holes at an injection speed of 17.2 m/min. The filaments were coagulated in a 1-m precipitation bath containing water and [EMIM][OAc] (80/20) at 40°C wound on electronically controlled godets at 8.0 m/min; they were then washed in water baths, dried, and finally processed for testing.

The 10 wt % cellulose solutions in [EMIM][OAc], [EMIM][DEP], and NMMO·H_2O, respectively, were extruded with a Fourné laboratory-scale piston spinning device. The fibers were

spun at 20–60°C with a spinneret with a hole diameter of 0.09 mm (length-to-diameter ratio = 0.72) containing 48 holes. The filaments were spun through a 10-mm air gap with an injection speed of 3.5 m/min, coagulated in a 1-m distilled water precipitation bath at 20°C, and wound on electronically controlled godets at 7.1 and 8.0 m/min to achieve jet draw ratios of 100 and 125%, respectively. Then, they were washed in water baths, dried, wound on a tension-controlled godet, and finally processed for analysis.

The ILs used for the processing of cellulose into fibers were recycled with a laboratory-scale device. The removal of the volatile component was accomplished by evaporation, which led to almost complete recovery of the solvent (>99.5%). Experiments regarding the recovery of NMMO were not performed in this study.

Viscometric Determination of the Degree of Polymerization (DP)

Changes in the DP of cellulose samples were investigated by the determination of the solution viscosities of ferric tartaric acid complexes in alkaline aqueous solutions (FeTNa) as they relate to molecular weight. The investigations were performed according to DIN 54270. The viscosity measurements were performed in a Ubbelohde viscometer with suspended-level bulb (type Ia) purchased from Schott Geräte GmbH. The average DP was calculated from the efflux time of the cellulose solution (t), the efflux time of the blank EWNN solution (t_0), and the concentration of cellulose in solution (c) according to the modified Schulz–Blaschke equation:

$$\mathrm{DP} = \frac{152 \cdot \eta_{\mathrm{spez}}}{c(1 + 0,339\eta_{\mathrm{spez}})}$$

where η_{spez} is the specific viscosity ($\eta_{\mathrm{spez}} = \eta_{\mathrm{rel}} - 1$) and η_{rel} is the relative viscosity ($\eta_{\mathrm{rel}} = t/t_0$).

Wide-Angle X-Ray Scattering (WAXS)

X-ray diffraction was accomplished by a Siemens PW 3710 $\theta/2\theta$ vertical goniometer with a texture grade. The wide-angle X-ray diffraction (WAXD) patterns were measured with Cu Kα [wavelength (λ) = 1.5405 Å] under continuous scanning at a rate of 0.01° 2θ/s at 35 kV and 150 mA.

The degree of crystallinity, crystallites dimensions, and orientation of the crystallites [Hermans' orientation factor (f_c)] were calculated with equatorial and meridional WAXS diffractograms. The calculation of crystallinity involved the measurement of equatorial wide-angle diffractograms. The degree of crystallinity was calculated on the basis of the following formula:

$$I_c = \frac{\sum I_c}{\sum (I_c + I_a)}$$

where I_c is the sum of the intensity of the crystalline reflections and I_a is the sum of the intensity of the amorphous reflections. The equatorial scan was separated into crystalline and amorphous reflexion by peak separation software with Pearson VII Concept.

The crystallite size (t) was calculated on the basis of Scherrer's formula according to the following equation:

$$t = \frac{K\lambda}{B\cos\theta_b}$$

where B is the width at half-height (integral breadth) of the reflection at 2θ and is corrected for the internal broadening of the equipment (~0.1°) for Lorentzian curves; K is the Scherrer factor, is dependent on the crystallite shape, and is equal to 1; and θ_B is the Bragg angle.

f_c was calculated according to the following equation:

$$f_c = \frac{3(\cos^2\theta_{hkl}) - 1}{2}$$

where θ_{hkl} is the angle between the longitudinal axis of the microfibrill of the crystallite and the preferred direction.

Birefringence (Δn)

Δn of the fiber samples was measured with a Leitz Laborlux polarizing microscope (12-pole-type Laborlux, 50/0.85 objective). The method was based on the determination of the phase difference [Γ_λ (indicated by $n_\parallel$ and $n_\perp$)] for monochromatic plane-polarized light in anisotropic materials. The diameter (d) of the fibers was obtained by a measuring scale situated in the eyepiece of the microscope. Δn was calculated by the following equation:

$$\Delta n = \frac{\Gamma}{d}$$

Morphology

Scanning electron micrographs were recorded with a Zeiss DSM 962. The samples were sputtered with Au/Pd before analysis.

Mechanical Textile Properties

The mechanical fiber properties were measured by means of a Textechno tensile tester at 20°C with an average of the results from 10 different fibers. The fineness was obtained as weight per 10.000 m in length. The gauge length was 25 mm, and the time to break was 20 s.

Water Retention Value (WRV)

The WRVs of the fibers were determined according to DIN 53814.

Fibrillation Behavior

The fibrillation behavior was determined by measurement of the mechanical friction of the fiber samples in the wet state. The 20-mm-long fiber samples were clamped within a polytetrafluoroethylene frame. The frames were placed in a 20.0-mL glass vessel with 9.0 g of zirconium oxide balls (0.8–1.0 mm in diameter, purchased from W. Hoffmann GmbH) and 2.5 mL of distilled water. They were heated to 30°C with a circulation rate of 50 rpm for 3 h with a Labomat. Finally, the morphology of the treated fibers was observed with an optical microscope at magnifications up to 50×.

RESULTS AND DISCUSSION

Dissolution Behavior

The Lyocell process was characterized by the direct dissolution of cellulose in NMMO and water. In this process, the pulp was first wetted with dilute aqueous NMMO (ca. 40% of H_2O),

Applied Polymer SCIENCE

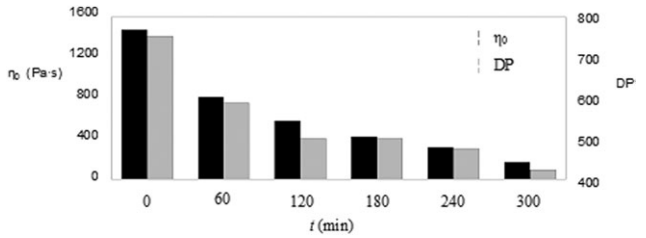

Figure 1. Dissolution behavior of the spinning dope: influence of the kneading time on the zero-shear viscosity (left *y* axis) and DP (right *y* axis) of 10 wt % cellulose in [EMIM][OAc] under oxygen (reference temperature = 85°C).

which caused a significant swelling of cellulose. Thereafter, excess water was distilled off from the solution at elevated temperatures until the desired ratios of cellulose/NMMO/water were obtained. The solution was stabilized by the application of a combination of alkaline and antioxidant stabilizers (NaOH, isopropyl gallate).

New technology using ILs for cellulose dissolution enables dope preparation either in a manner very similar to the NMMO process by disintegrating the pulp in aqueous IL followed by removing the excess water *in vacuo* and heating or direct dissolution in a kneader.[30,31,47] Because the latter dissolution technique has big advantages under laboratory conditions, such as mild dissolution conditions (85°C, 1.01 bar) and economically advantageous processing times of 1–2 h, the preparation of cellulosic solutions in ILs in this study was performed according to the direct dissolution process.

The dissolution behavior of cellulose in IL was of fundamental importance for its processing (Figure 1). Therefore, analytical investigations of the dissolution process of cellulose with ILs were made by analysis of the rheological properties of the solutions along with the viscometric determination of the molecular weight of each regenerated sample by hourly sampling.

These investigations showed that the viscosity of the spinning dope and the DP of the pulp could be tailored to optimize the dope preparation; this allowed greater variability in the proximate spinning procedure. Although the dissolution process in ILs under an oxygen atmosphere is accompanied by alteration reactions involving the oxidative degradation of cellulose over time, the preparation of cellulose solutions in the presence of

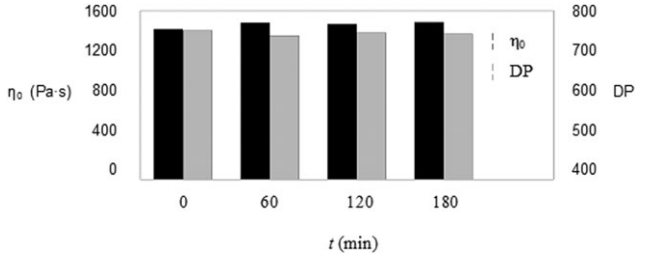

Figure 2. Dissolution behavior of the spinning dope: influence of the kneading time on the zero-shear viscosity (left *y* axis) and DP (right *y* axis) of 10 wt % cellulose in [EMIM][OAc] under nitrogen (reference temperature = 85°C).

Table I. Dissolution of Wood Pulp According to the NMMO Process and with ILs

	NMMO process	IL processes	
Solvent	NMMO·H_2O	[EMIM][OAc]	[EMIM][DEP]
Dope concentration (wt %)	10.0	6.0 and 10.0	10.0
Water content (wt %)	≤13.3	≤5.0	≤5.0
Stabilization	+	–	–
Dissolution conditions			
Temperature (°C)	120.0	85.0	85.0
Pressure (bar)	0.02	1.01	1.01
Time (h)	4–5	1–2	1–2

–, without stabilizer; +, with stabilizer.

an inert gas atmosphere (N_2) maintained consistent rheological properties of the spinning dope and a nearly unchanged DP. The results also reveal that the dissolution of cellulose in ILs under an inert atmosphere occurred without degradation (Figure 2).

To compare the dissolution behavior and the processing parameters for cellulose in 6 and 10 wt % NMMO·H_2O, [EMIM][OAc], and [EMIM][DEP] spinning dopes were made and characterized through both wet- and dry–wet-spinning processes. The parameters used for the production of the spinning dopes are summarized in Table I.

Rheological Behavior of the Spinning Dopes

The experimental parameters for the processing of cellulose solutions were chosen according to theoretical considerations made by Ziabicki.[48] To characterize the window of spinnability, the rheological properties of the spinning dopes were studied over a wide range of concentrations and temperatures (Figure 3).

A comparison of the rheological properties of cellulose solutions in ILs with those in NMMO indicated that strong similarities in

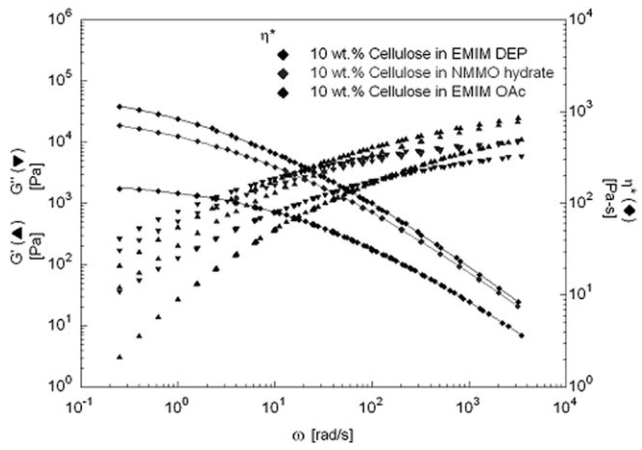

Figure 3. Rheological behavior of the 10 wt % cellulosic solutions in [EMIM][OAc], [EMIM][DEP], and NMMO·H_2O at 100°C.

Table II. Spinning Parameters of the Dopes by Means of the Wet- and Dry–Wet-Spin Processes

Processing	Wet spinning	Dry–wet (air gap) spinning		
Solvent	[EMIM][OAc]	[EMIM][OAc]	[EMIM][DEP]	NMMO·H_2O
Dope concentration (wt %)	6.0	10.0	10.0	10.0
Spinning temperature (°C)	90.0	20.0	60.0	55.0
η_0 (Pa s)[a]	38.6	144.6	1135.5	705.4
η_0 (Pa s)[b]	32.9	1.8×10^4	1.8×10^4	1.8×10^4
Nozzle aperture (μm)	40.0	90.0	90.0	90.0
Number of holes	1000	48	48	48
Air gap (mm)	—	10.0	10.0	10.0
Jet draw ratio (%)	−50	100/125	100/125	100/125
Precipitation bath	Water/[EMIM][OAc]	Water	Water	Water

[a]Determined by the construction of temperature-independent master curves at 100°C.
[b]Determined by rheological measurements at the spinning temperature used.

the rheological behavior existed, despite the different dissolution methods. The characteristics of the shear viscosity and the dynamic moduli of both the NMMO-based and IL solutions were almost identical. However, the results regarding the viscosities of cellulose solutions in NMMO·H_2O and [EMIM][DEP], respectively, corresponded to essentially greater values than the results using concentrated solutions in [EMIM][OAc]. Because of the superior dissolving capability of ILs for cellulose, the flow behavior of the spinning dopes in [EMIM][OAc] differed drastically from those in NMMO·H_2O and [EMIM][DEP] and, therefore, required different processing parameters.

The processing of cellulose by dissolution in ILs has some considerable advantages over the NMMO process. Low-viscosity cellulosic solutions in [EMIM][OAc] were processed by means of a standard wet-spinning process in a concentration range between 5 and 8 wt %. Furthermore, concentrated spinning dopes (≥10 wt %) were converted to fibers in both [EMIM][OAc] and [EMIM][DEP] with the dry–wet-spinning process.

The wet-spinning process was limited by shearing forces in the spinneret and, therefore, was determined by the viscosity of spinning dope and the actual velocity gradient in the coagulation bath. The situation was more complicated when dry–wet spinning was considered. The spinning process became sensitive to both the viscosity and rheological flow behavior, as defined by the elastic and viscous moduli. To characterize the window of spinnability, the rheological properties of the spinning dopes were studied between 20 and 100°C. Then, the flow behavior of the spinning dopes was adjusted by temperature to the same viscosity to produce identical course of curves of G' and G''. As mentioned previously, the processing parameters with an air gap in [EMIM][OAc] differed drastically from those in NMMO·H_2O and [EMIM][DEP]; this made comparison under equal processing conditions difficult.

Additionally, the ILs were liquid over a wide temperature range and were soluble in most organic solvents; this led to various options with regard to the coagulation process, such as the temperature control of the spinning dope and variety in the precipitation medium. The process directions within the NMMO process compared to the IL technology were explicitly limited. Particularly, the relatively high melting point of NMMO·H_2O (74°C) and the instability of cellulosic solutions in NMMO·H_2O played a decisive role. Because of the numerous side reactions and appreciable byproduct formations in the system involving cellulose/NMMO/water in the Lyocell process, the solutions had to be stabilized by compounds such as propyl gallate. In contrast to the Lyocell process, the dissolution of cellulose in ILs was performed under mild conditions. Because a stabilization of the dope was not necessary, a high recovery of the solvent was possible, and a consistent fiber performance was the result.

Spinning Trials

The spinning parameters for fiber production with wet and dry–wet processing techniques are summarized in Table II.

Structure and Properties of the Produced Fibers

The structure of the cellulosic fibers was defined by molecular, supramolecular, and morphological structure parameters and by the pore formation and the fiber's inner surface.[5] These fiber parameters, their relationship, and the resulting physical textile properties were all influenced by the processing technique.[49]

Molecular and Supramolecular Structure

Viscometric investigations regarding the molecular structure of man-made cellulosic fibers showed that the average molecular weight of cellulose depended on the solution processing, and the fibers exhibited DP values between 500 and 590 when dissolved pulp with an original DP value of 592 was used. The 6 wt % spinning dopes in [EMIM][OAc] exhibited quite low viscosities and, therefore, could be degassed within a few hours. The deaeration of highly viscous spinning dopes in [EMIM][OAc] for dry–wet processing required several days at elevated temperatures. These extreme conditions caused cellulose degradation, which, however, did not significantly influence the processing technique and the final fiber performance.

The characterization of the supramolecular structure of the fibers included WAXS and Δn.[50] The crystallite size and the percentage crystallinity were calculated on the basis of an

Table III. Structural Data of the Produced Cellulosic Fibers

Solvent	DP[a]	Crystallinity[b]	Elementary fibril		Chain orientation[d]	
			Crystallite width (nm)[c]	Crystallite length (nm)[d]	f_c[e]	Δn
Wet spinning						
[EMIM][OAc]	590	Low				0.02665
Dry–wet spinning[a]						
[EMIM][OAc]	500	High	3.15	8.62	0.814	0.03534
[EMIM][DEP]	524	High	3.33	5.87	0.788	0.03550
NMMO·H_2O	556	High	3.23	6.14	0.769	0.03668

[a]Jet draw ratio = 100%. Original $DP_{(FeTNa)}$ = 592.
[b]High > 85%. Low < 85%.
[c]Derived from the 101 reflection.
[d]Derived from the 004 reflection.
[e]f_c = 1, perfect orientation; f_c = 0, isotopic angular distribution.

equatorial and meridional X-ray scan of the fiber samples, and thus, the values displayed in Table III depended on the concentration of crystallinity only in the equatorial slice and not in the entire halo. Thus, these values did not represent an absolute percentage crystallinity throughout the sample due to the isotropic fiber properties, but they were comparable to each other. Therefore, only the crystallinity data via X-ray are quoted.

The crystallite size and percentage crystallinity varied with the solvent system and the jet draw ratio. Because of the low crystalline order of the wet-spun fibers, the reliable X-ray data were inconclusive in this case. The results of the X-ray analysis of the fibers with different solvent systems for dry–wet spinning showed that the crystallites aligned perpendicularly to the chain direction exhibited uniform dimensions. However, there were noticeable differences in the sizes of the crystallites parallel to the chain direction. The assessed data reflected the influence of the anion of the ILs on the dimensions of the crystallites. A combination of a comprehensive evaluation of the X-ray data with the results obtained by Δn showed that there were no differences in the total chain orientation values or in the orientational state of the crystallites between the dry and wet manufactured fibers. The results of the investigations show that the application of various solvent systems for cellulose processing had a substantial influence on the supramolecular structure of the fibers produced. Particularly, the influence of the anion of the ILs on the cellulose regeneration process in the coagulation bath seemed to play a very important role in the kinetics of solidification. In comparison to the soft diethyl phosphate anions, the harder acetate anions affected different interactions between the coagulation agent and the spinning solution; this led to the formation of longer crystallites when [EMIM][OAc] was used.

Morphological Structure

The morphological structure of the fibers was investigated with electron microscopy. The prepared fibers revealed no significant differences in the fiber cross sections with regard to the fibrillar and void morphology. Because of the rapid coagulation, all of the fibers showed an almost round profile, a smooth surface, and no visible differences. The profile of the cross section of the wet-spun fiber was very homogeneous, and no fibrillar aggregates could be determined. In case of the dry–wet-spun fibers, a similar morphological structure was observed, despite the application of different solvent systems. The dry–wet-spun fibers showed a similar, mostly fibrillar network structure, which was due to the high orientation of the fibers obtained after the air gap (Figures 4–7).

Physical Textile Properties

The mechanical fiber properties and the end-use properties of the fabrics were closely related to the fiber structure.[5,49] The physical fiber properties mainly depended on the molecular and supramolecular structure. A further important parameter was the morphology of the fiber and its inner surface and pore formation.

Important physical textile properties of commercially available man-made cellulosics in comparison to cotton were summarized by Bredereck and Hermanutz.[5] The values obtained for the tenacity and elongation were slightly lower compared to those of commercially available cellulosic fibers. The spinning trials did not completely exhaust the potential of processing techniques because the spinning dopes were processed on laboratory-scale equipment. Therefore, certain parameters could not be

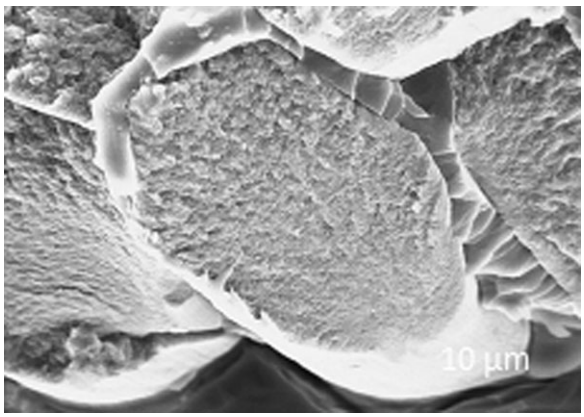

Figure 4. Scanning electron micrograph of the wet-spun fiber sample from [EMIM][OAc].

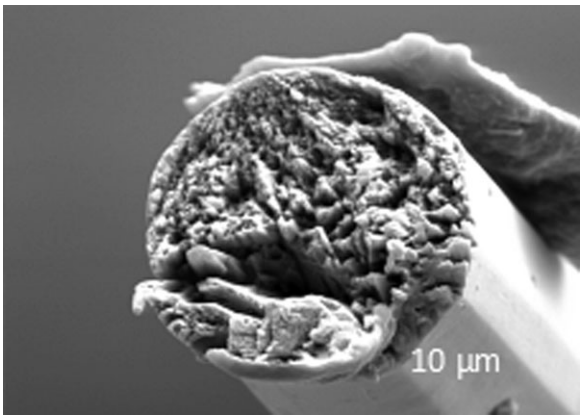

Figure 5. Scanning electron micrograph of the dry–wet-spun fiber sample from [EMIM][OAc].

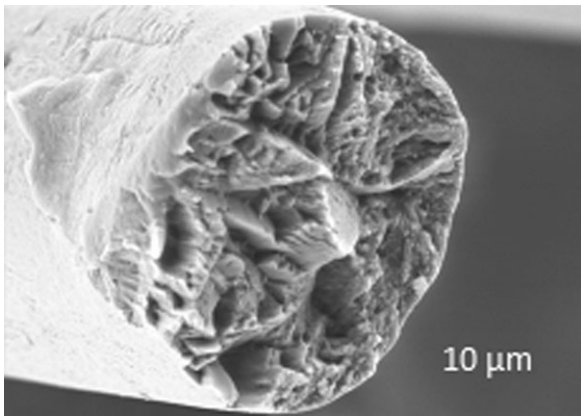

Figure 7. Scanning electron micrograph of the dry–wet-spun fiber sample from [EMIM][DEP].

optimized. Nevertheless, the spinning trials were reproducible and suitable for the precise investigation of various parameters with regard to the structure and properties of cellulosic fibers.

A comparison of NMMO fibers with samples spun from ILs led to the conclusion that their physical textile properties were quite similar. The data obtained suggest that the similar homogeneous dissolution state of the spinning dopes exhibited similar structures as the resulting fibers. The fibers obtained by means of the wet-spinning procedure exhibited tensile strengths of approximately 22 cN/tex and elongations at break of 8% under dry conditions. The resulting mechanical properties of the fibers in the dry–wet-spinning process of the cellulose solutions in NMMO hydrates and ILs ranged from 25 to 26 cN/tex with regard to tensile strength and from 4 to 9% in terms of elongation at break. Also, the tensile curves of the dry–wet-spun fibers possessed almost identical characteristics within the range of low elongation.

Water Retention Values (WRVs)

The empirical measure of the water-holding capacity for cellulosic fibers involved the determination of the weight ratio of water retained after centrifugation under specified conditions by a wet fiber sample to the weight of the same at 105°C dried fiber samples. The WRV depends on the supramolecular and morphological structure and was essentially limited to the amorphous structural regions and the void system of the cellulosic fibers.

The results of the investigation with regard to water retention show that the absorption behavior of the fibers was clearly affected by the spinning process.[5,51] The low-crystalline, wet-spun fibers showed significantly higher water retention values compared to those spun with an air gap. The high-crystalline, dry–wet-spun fibers exhibited only small differences in the water retention with different solvent systems.

Fibrillation Behavior

A special property of Lyocell fibers is their distinct fibrillation behavior in the wet state, which is derived from their fiber structure, which contains long, highly oriented crystallites and low lateral interactions between the fibril bundles (Figures 8–11).[5,21–23]

The fibrillation behavior of the produced fibers was studied by the subjection of the fiber samples to chafing damage in the wet state, followed by microscopic examination. As expected, the results show that the wet-spun fibers have the lowest tendency toward fibrillation. The wet-spun samples did not show any splitting of the fibrillar elements at the fiber surface. The low tendency of the fiber fibrillation could be explained by low crystallinity and small orientation of these fibers. However, clear

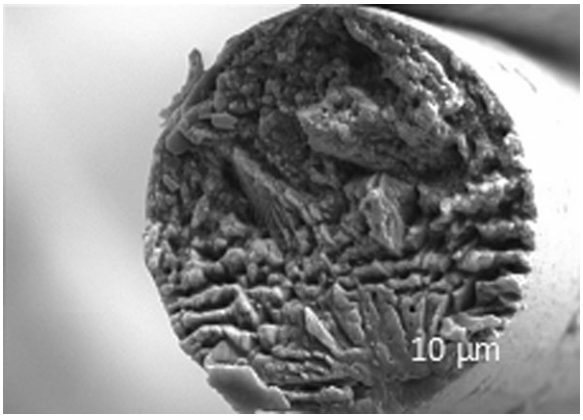

Figure 6. Scanning electron micrograph of the dry–wet-spun fiber sample from NMMO·H_2O.

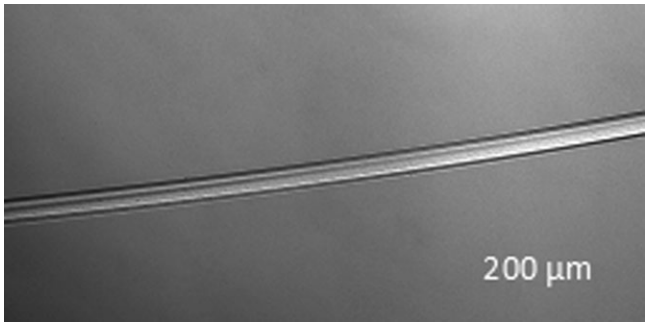

Figure 8. Micrograph of the wet-spun fiber sample from [EMIM][OAc] (jet draw ratio = 50%).

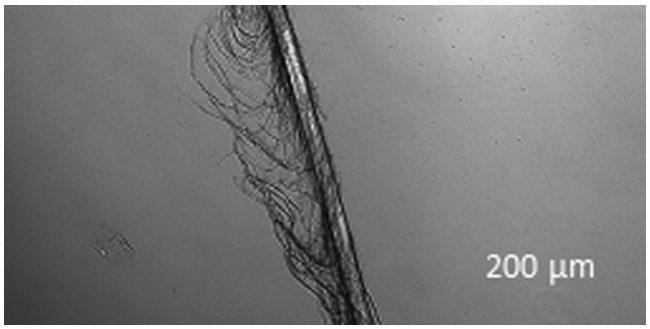

Figure 9. Micrograph of the dry–wet-spun fiber sample from [EMIM][OAc] (jet draw ratio = 125%).

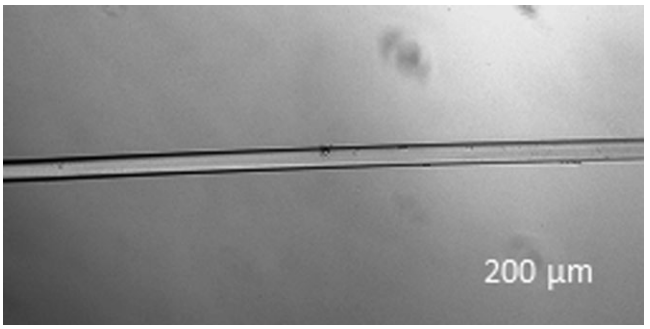

Figure 11. Micrograph of the dry–wet-spun fiber sample from [EMIM][DEP] (jet draw ratio = 125%).

differences in the fibrillation behavior were served for the dry–wet spun fibers. Although the [EMIM][DEP] processed fibers had almost no tendency to fibrillate, the samples spun from [EMIM][OAc] showed a significant fibrillating tendency in the wet state. The NMMO-based fiber could be classified with regard to fibrillation behavior between the two IL spun samples. The fibrillation tests showed that both application of various processing techniques and the use of different solvent systems had a substantial influence on the supramolecular structure and the physical textile properties of the fibers produced. In this regard, the results of the fibrillation tests confirmed the WAXD measurements well. It follows from theory of the structure and properties of cellulosic fibers that the formation of the supramolecular structure with long crystallites was associated with a low crosslinking of the crystalline regions and led to a higher tendency of the fiber to fibrillation. Although the dry–wet-spun fibers with [EMIM][DEP] with small crystalline domains showed the lowest tendency toward fibrillation, the [EMIM][OAc] dry–wet-spun fibers had long crystalline regions and, therefore, a strong tendency to fibrillate in the wet state.

CONCLUSIONS

Today, the production of regenerative cellulosic fibers is performed almost exclusively by the viscose and Lyocell process. The advantage of the viscose process is the high tunability of the spinning conditions, which results in a large and a variable range of targeted fiber properties. Disadvantages of the viscose process include not only the time-consuming preparation of the alkali-soluble cellulose xanthate but also the handling of toxic and easily inflammable carbon disulfide, high water consumption, and contamination of the atmosphere and the process water with sulfur compounds during coagulation. The contamination of the coagulation bath with huge amounts of sodium and zinc salts requires further cost-intensive investment in pollution-control systems.

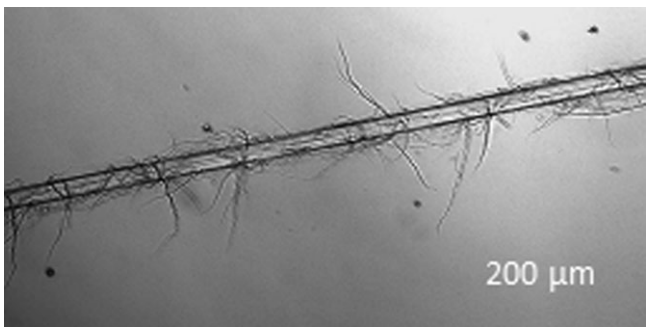

Figure 10. Micrograph of the dry–wet-spun fiber sample from NMMO·H_2O (jet draw ratio = 125%).

The Lyocell process is characterized by the direct dissolution of cellulose in NMMO·H_2O and the possibility of producing high-strength fibers. One severe disadvantage of Lyocell fibers is their strong tendency to undergo wet fibrillation. Moreover, the solvent NMMO is thermally unstable, not miscible with organic solvents, and only miscible with water in a very limited range. ILs, which have become easily available in recent times, are also able to dissolve cellulose directly. They are, however, thermally absolutely stable and can be used for the spinning of regenerative cellulosic fibers in water as coagulant. NMMO, in principle, can be considered an intramolecular IL. However, in contrast to NMMO, a variation of anions in ILs is possible, whereby the properties of the fibers obtained can be changed considerably.

In this study, we demonstrated the enormous influence of anions in ILs on the spinning process and the properties of the produced regenerated cellulosic fibers. In the dry–wet-spinning process (e.g., see Table IV), the textile mechanical properties of the prepared fibers, spun in [EMIM][OAc], [EMIM][DEP], and NMMO·H_2O, respectively, were absolutely comparable, but the fibrillation behavior (Figures 9–11) was totally different. The dry–wet-spun fiber sample from [EMIM][DEP] (Figure 11) showed practically no fibrillation tendency in contrast to the fiber spun from NMMO·H_2O (Figure 10). With ILs as solvents, a wet-spinning process, comparable to that in the viscose method, was possible. With [EMIM][OAc] as a solvent, fibers with the lowest tendency of fibrillation were obtained (Figure 8). In addition, with regard to the processing technique, ILs have many advantages over NMMO·H_2O as solvents for cellulose. These include stable nontoxic solvents, which can be recycled almost completely (>99.5%), the application of various processing techniques with a substantial influence on the supramolecular structure, and the physical textile properties of the fibers produced. Because IL process technology enables the spinning of cellulose with various techniques with different ILs, the resulting fiber property profiles differed significantly, depending on the process parameters chosen. Because of the many

Table IV. Physical Textile Values of the Manufactured Fibers

Solvent	Fineness (dtex)	Tenacity (cN/tex)		Elongation (%)		WRV (%)	Fibrillation[b]
		CD[a]	Wet	CD[a]	Wet		
Wet spinning							
[EMIM][OAc]	1.6	22.2	19.6	8.0	9.8	101.0	–
Dry-wet spinning[a]							
[EMIM][OAc]	4.1	24.6	21.4	3.8	5.2	78.6	++
[EMIM][DEP]	4.9	26.4	23.9	6.0	6.6	87.3	–
NMMO·H_2O	4.7	25.9	23.1	8.5	9.7	79.5	+

Jet draw ratio = 100%. CD, conditioned dry (65% relative humidity, 20°C); –, very low fibrillation tendency; +, high fibrillation tendency; ++, very high fibrillation tendency.

advantages of IL technology, further applications of IL-based cellulose processes, such as nonwovens, blow extrusion films, coatings, and microbeads, will become possible and interesting.

REFERENCES

1. Klemm, D.; Fink, H.-P. *Angew. Chem.* **2005**, *117*, 3422.
2. Anastas, P. T. Handbook of Green Chemistry; **2009**; Vol. *6*.
3. Rogers, R. D.; Seddon, K. R. Ionic Liquids as Green Solvents: Progress and Prospects; **2003**; p 14.
4. Klemm, D.; Philipp, B.; Heinze, T.; Heinze, U.; Wagenknecht, W. Comprehensive Cellulose Chemistry; Wiley-VCH: **1998**; Vol. *1*.
5. Bredereck, K.; Hermanutz, F. *Rev. Prog. Color.* **2005**, *35*, 59.
6. Gross, A. S.; Chu, J.-W. *J. Phys. Chem. B* **2010**, *114*, 13333.
7. Cho, H. M.; Gross, A. S.; Chu, J.-W. J. *J. Am. Chem. Soc.* **2011**, *133*, 14033.
8. Lindman, B.; Karlström, G.; Stigsson, L. *J. Mol. Liq.* **2010**, *156*, 76.
9. Rogowin, Z. A.; Chemiefasern, G. Thieme Verlag, **1982**.
10. Neupert, A.; et al. Textile Faserstoffe; VEB Fachbuchverlag, **1961**.
11. Turbak, A. Encyclopedia of Polymer Science and Engineering; Wiley: New York, **1988**; Vol. *14*.
12. Woodings, P. Regenerated Cellulose Fibres; Woodhead: Cambridge, England, **2000**; p 1.
13. Albrecht, W.; Reintjes, M.; Wulfhorst, B. *Chem. Fibers Int.* **1997**, *47*, 298.
14. Schleicher, H.; Fink, H.-P. *Lenzinger Ber.* **1994**, *9*, 5.
15. Michels, C.; Kosan, B. *Lenzinger Ber.* **2001**, *80*, 13.
16. Loubinoux, D.; Chaunis, S. *Text. Res. J.* **1987**, *57*(2), 61.
17. Chanzy, H.; Paillet, M.; Hagege, R. *Polymer* **1990**, *31*, 400.
18. Perepelkin, K. E. *Fibre Chem.* **2007**, *39*, 163.
19. Kim, D. B.; Pak, J. J.; Jo, S. M.; Lee, W. S. *Text. Res. J.* **2005**, *75*, 331.
20. White, P. Regenerated Cellulose Fibres; Woodhead: Cambridge, England, **2000**; p 62.
21. Ortlepp, G.; Beckmann, E.; Mieck, K. P. *Chem. Fibers Int.* **1996**, *46*, 63.
22. Kampl, R.; Leitner, H. *Lenzinger Ber.* **1996**, *75*, 97.
23. Mieck, K. P.; Nikolai, A. *Lenzinger Ber.* **1994**, *74*, 73.
24. Rosenau, T.; Potthast, A.; Sixta, H.; Kosma, P. *Prog. Polym. Sci.* **2001**, *26*, 1763.
25. Buijtenhuys, F. A.; Abbas, M.; Witteveen, A. I. *Papier* **1986**, *40*, 615.
26. Wachsmann, U.; Diamantoglou, M. *Papier* **1997**, *51*, 660.
27. Wendler, F.; Konkin, A.; Heinze, T. *Macromol. Symp.* **2008**, *262*, 72.
28. Wendler, F.; Kolbe, A.; Kraft, J.; Einax, J. W.; Heinze, T. *Macromol. Theory Simul.* **2008**, *17*, 32.
29. Swatloski, P.; Spear, S. K.; Holbrey, J. D.; Rogers, R. D. *J. Am. Chem. Soc.* **2002**, *124*, 4974.
30. Hermanutz, F.; Massonne, K.; Uerdingen, E. *Chem. Fibers Int.* **2006**, *6*, 342.
31. Hermanutz, F.; Gähr, F.; Meister, F.; Kosan, F.; Uerdingen, E. Presented at Cellulose-Symposium at Wiesbaden, Germany, **2007**.
32. Vagt, U. *CHEManager* **2008**, *22*, 19.
33. Stegmann, V.; Massonne, K.; Maase, M.; Uerdingen, E.; Lutz, M.; Hermanutz, F.; Gähr, F. U.S. Pat. 0269477 A1 (**2008**).
34. Greaves, T. L.; Drummond, C. *J. Chem. Rev.* **2008**, *108*, 206.
35. Schlottenberger; Sixta; et al. *Am. Chem. Soc. Symp. Ser.* **2010**, *1033*, 229.
36. Wang, H.; Gurau, G.; Rogers, R. D. *Chem. Soc. Rev.* **2012**, *41*, 1519.
37. Heinze, T.; Dorn, S.; Schöbitz, M.; Liebert, T.; Köhler, S.; Meister, F. *Macromol. Symp.* **2008**, *262*, 8.
38. Gericke, S. K.; Liebert, T.; Heinze, T.; Budtova, T. *Biomacromolecules* **2009**, *10*, 1188.
39. Pinkert, A.; Marsh, K.; Pang, S.; Staiger, M. P. *Chem. Rev.* **2009**, *109*, 6712.
40. Winterton, N. *J. Mater. Chem.* **2006**, *16*, 4281.
41. Garcia, M. T.; Gathergood, N.; Scammells, P. *J. Green. Chem.* **2005**, *7*, 9.

42. Sowmiah, S.; Srinivasadesikan, V.; Cheng, M.-C., Chu, Y.-H. *Molecules* **2009**, *14*, 3780.

43. Massonne, K.; Siemer, M.; Mormann, W.; Leng, W. Pat. DE102007041416A (**2009**).

44. King, A. W. T.; Asikkala, J.; Mutikainen, I.; Järvi, P.; Kilpeläinen. *Angew. Chem. Int. Ed.* **2011**, *50*, 6301.

45. Röder, T.; Moosbauer, J.; Kliber, G.; Sixta, H. Presented at the 8th International Symposium Alternative Cellulose-Symposium, Rudolstadt, Germany, **2008**.

46. Cai, T.; Zhang, H.; Guo, Q.; Shao, H.; Hu, X. *J. Appl. Polym. Sci.* **2010**, *115*, 1047.

47. Wendler, F.; Kosan, B.; Krieg, M.; Meister, F. *Lenzinger Ber.* **2009**, *87*, 106.

48. Ziabicki, A. Fundamentals of Fibre Formation; Wiley-Interscience, **1976**.

49. Schurz, J. *Lenzinger Ber.* **1994**, *9*, 37.

50. Falkei, B. V. Synthesefasern; Verlag Chemie: **1981**.

51. Testing of Textiles: Determination of Water Retention Power of Fibres and Yarn Cuttings; DIN 53814; Deutsches Institut Fur Normung: **1974**.